Mobile Networks and Applications
https://doi.org/10.1007/s11036-020-01545-z

Linearization of RF Power Amplifiers in Wideband Communication Systems by Adaptive Indirect Learning Using RPEM Algorithm

Duc Han Le[1] · Van-Phuc Hoang[1] · Minh Hong Nguyen[1] · Hien M. Nguyen[2] · Duc Minh Nguyen[3]

Abstract
This paper proposes a new approach of digital predistortion (DPD) technique based on the adaptive indirect learning architecture (ILA) by using a recursive prediction error minimization (RPEM) algorithm for linearizing radio frequency (RF) power amplifiers (PAs) in emerging wideband communication systems. In the proposed RPEM-based linearization approach, the forgetting factor varies with time and is less sensitive to noise. Therefore, the predistorter (PD) parameter estimates become more consistent and accurate in steady state so that the mean square errors can be reduced. Both the error vector magnitude (EVM) and the adjacent channel power ratio (ACPR) are used to evaluate the DPD technique in RF PAs employing the proposed linearization. The efficiency validation of the proposed method is based on a simulated PA Wiener model. The simulation results have clarified the improvement of the proposed adaptive ILA-based DPD with RPEM algorithm in terms of both EVM and ACPR.

Keywords RPEM · Digital predistortion · RF power amplifiers · Linearization · Adaptive indirect learning architecture · Predistorter

1 Introduction

The development of future wireless communication systems, such as the fifth generation (5G) and beyond [1, 2], continuously demands higher data rates and larger user capacities, which faces significant challenges in both system performance and energy efficiency. It requires not only wideband transceiver architecture, but also higher-order modulation schemes. The signals of these systems are characterized by non-constant envelopes and high peak-to-average power ratio (PAPR), leading to stringent linearity requirements for signal amplification. In the meantime, the power dissipation must be remained as low as possible. To cope with these challenges, high efficiency and linear radio frequency (RF) power amplifiers (PAs) are indispensable components. Unfortunately, due to the inherent nonlinear behavior of PAs, efficiency and linearity requirements often conflict each other. In order to provide highly-efficient power conversion, PAs should be driven into the saturation region. However, the saturated PAs produce not only in-band distortion but also result in spectral regrowth that interferes the adjacent frequency band channels. Consequently, the spectra utilization efficiency is reduced. In contrast, the nonlinear distortion can be mitigated by a traditional back-off approach, but this generates low power efficiency due to the high PAPR of the transmitted signals. In order to maintain a low level of distortion without sacrificing the system energy efficiency requirement, PA linearization techniques are often used [3].

Thanks to its flexibility and excellent linearization performance, the baseband digital predistortion (DPD) has been recognized as one of the most cost-effective linearization techniques [4–10], and it also tends to be popularly and widely used in wireless transmitters for the next generation wireless communication systems. In this scheme, a predistorter (PD) block is placed in front of a PA. The PA input signal is pre-distorted by the PD whose transfer function is the inverse of that of the PA. Ideally, the cascade of the PD and PA behaves as a linear amplification system and the original input is amplified by a constant gain.

This paper has been submitted in part to the 5th EAI International Conference on Industrial Networks and Intelligent Systems (INISCOM 2019). The corresponding and the first authors are the main authors contributing equally to the paper.

✉ Van-Phuc Hoang
phuchv@lqdtu.edu.vn

Extended author information available on the last page of the article.

In practice, the PA characteristics change with time due to process, supply voltage, and temperature (PVT) variations. In order to track time-varying change in the PA characteristics, an adaptive DPD, using cost-effective learning architectures, has become one of the most preferred choices. There are two commonly and widely used learning architectures for PD parameter identification: indirect learning architecture (ILA) [11–13] and direct learning architecture (DLA) [9, 10, 14, 15]. Although DLA is more robust than ILA in terms of noise at the PA output and can provide unbiased parameter estimates, it is more complex identification process since the adaptive algorithms used in DLA require many iterations to find a set of parameters that minimizes the optimization criterion [4]. For these reasons, the adaptive ILA is most often used for identifying the PD parameters in RF PAs [4].

The existing DPD systems are mainly used for the scenarios where the PAs operate under relatively stable conditions, e.g., the PA characteristics remain almost constant over time [6, 16]. As the PA characteristics change over time, authors in [17] developed the adaptive ILA using least mean squares (LMS) for linearizing PAs, herein denoted as LMS-ILA for simple presentation. The main advantage of LMS is its simple implementation. However, it provides inaccurate estimation and has slow convergence since increasing the step size parameter leads instability problems. Moreover, it is also sensitive to the scaling of the input signal, making it very hard to choose a proper step size [17]. In order to obtain faster convergence of the adaptation, authors in [11, 13] proposed the adaptive ILA using recursive least squares (RLS) that is here denoted as RLS-ILA to simplify the presentation. It is worth noting that the choice of forgetting factor λ is often essential to make a good trade-off between the convergence and accuracy. For RLS, a decrease in the forgetting factor λ leads to its sensitivity to noise and a larger fluctuation of parameter estimates [18], resulting in inefficiency linearization performance. With the continuous development of the wideband communication systems, more efficient linearization methods for RF PAs are desired to meet the emerging requirement of highly linear PAs in these systems. On the other hand, the recursive prediction error method (RPEM) has shown its advantage to overcome the above issue of RLS-ILA linearization approach thanks to its time-varying forgetting factor λ [18].

Therefore, based on the above review on existing methods for linearizing RF PAs in wideband communication systems, in this paper, we propose a new approach of adaptive ILA using recursive prediction error method (RPEM) to linearize PAs operating under the time-varying condition. Thanks to its time-varying forgetting factor λ, the RPEM algorithm reduces the fluctuation of the PD parameter estimates, increase the convergence speed, mitigates the steady-state mean square error and hence minimizes the total nonlinear distortion at the PA output. In other words, the proposed predistortion technique allows us to reduce the nonlinear distortion adaptively without causing instability, and to solve several problems that arise when using either LMS-ILA or RLS-ILA. As a result, the adaptive ILA with RPEM effectively compensate the nonlinear distortion of the PA even if the PA characteristics changes due to PVT drift and other factors such as type of signals, high-order modulation schemes and input power levels.

The rest of the paper is organized as follows. Section 2 develops the adaptive ILA linearization using LMS or RLS, then proposes the one using RPEM and presents the figures of merit for performance evaluation. The detail simulation results and discussions are presented in Section 3. Conclusions are finally included in Section 4.

2 Proposed adaptive ILA-based linearization of RF power amplifiers with RPEM algorithm

2.1 Prediction error

Figure 1 shows the block diagram of the ILA-based DPD technique, where a post-distorter (or training) block is used to identify the postinverse of the PA. The baseband signal $u(n)$ is fed to the predistorter, which generates a signal $x(n)$ that is a PA input. The PA output signal is normalized by a linear gain G_0, producing the normalized output $z(n)$, i.e., $z(n) = \frac{y(n)}{G_0}$. The postdistorter model has the input $z(n)$ and the output $z_p(n)$. Its parameters are identified by minimizing the error signal $e(n) = x(n) - z_p(n)$ using the adaptive algorithms. Note that both the PD and postdistorter models are identical. Thus, when the coefficients of the postdistorter are identified, they are directly copied to the PD model. This process is repeated iteratively until the ILA linearization has

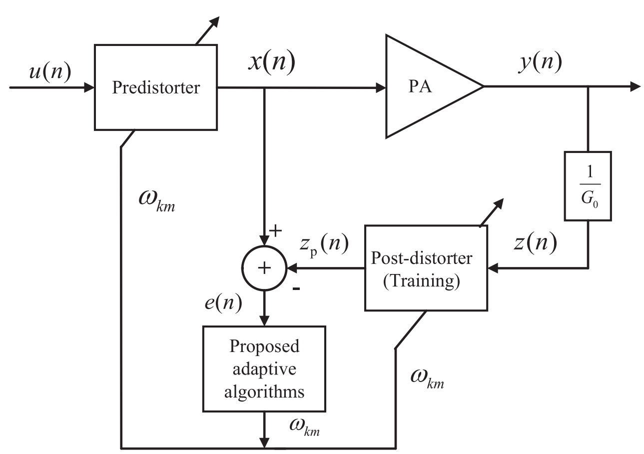

Fig. 1 Block diagram of Indirect learning architecture (ILA) using the proposed adaptive algorithms

converged. At convergence, the cascaded PD and PA system behaves linearly. Since the Memory Polynomial (MP) models have owned low computational cost, satisfactory accuracy, and easy hardware implementation, they have become one of promising choices and been widely applied for behavioral modeling and predistortion of PAs exhibiting nonlinear memory effects [3, 5, 13, 19]. Therefore, both the PD and postdistorter are modeled by the same MP model that has Q as the nonlinearity order and P as memory depth, and ω_{km} as coefficients. The input and output relation of the PD model is given by

$$x(n)=\sum_{k=1}^{Q}\sum_{m=0}^{P}\omega_{km}u(n-m)|u(n-m)|^{k-1}=\omega^{T}\phi(n), \quad (1)$$

where

$$\omega=\left[\omega_{10},\ldots,\omega_{Q0},\ldots,\omega_{1P},\ldots,\omega_{QP}\right]^{T}, \quad (2)$$

and

$$\phi(n)=\left[\phi_{10}(n),\ldots,\phi_{Q0}(n),\ldots,\phi_{1P}(n),\ldots,\phi_{QP}(n)\right]^{T} \quad (3)$$

with

$$\phi_{km}(n)=u(n-m)|u(n-m)|^{k-1}. \quad (4)$$

In the above equations, the symbol T indicates the matrix transpose.

The input and output of the postdistorter model can be expressed by

$$z_{\mathrm{p}}(n)=\sum_{k=1}^{Q}\sum_{m=0}^{P}\omega_{km}z(n-m)|z(n-m)|^{k-1}=\omega^{T}\mathbf{z}(n), \quad (5)$$

where ω is defined as in (2) and

$$\mathbf{z}(n)=\left[z_{10}(n),\ldots,z_{Q0}(n),\ldots,z_{1P}(n),\ldots,z_{QP}(n)\right]^{T} \quad (6)$$

with

$$z_{km}(n)=z(n-m)|z(n-m)|^{k-1}. \quad (7)$$

The prediction error $e\,(n,\omega)$ is defined by

$$e\,(n,\omega)=x(n)-z_{\mathrm{p}}(n)=x(n)-\omega^{T}\mathbf{z}(n). \quad (8)$$

The adaptive algorithms are derived by minimizing corresponding lost functions that refer to scalar-valued functions of all the prediction error values $e\,(n,\omega)$.

2.2 Development of the adaptive ILA linearization using LMS or RLS

The LMS algorithm is derived by minimizing the mean square error (MSE) $E\left\{e^{2}(n,\omega)\right\}$, where E denotes the expected values. It is obtained by applying the following stochastic gradient algorithm as in [20, 21].

$$\begin{aligned}\omega^{T}(n)&=\omega^{T}(n-1)-\frac{1}{2}\mu\frac{\partial e^{2}(n,\omega)}{\partial\omega}\\&=\omega^{T}(n-1)+\mu e(n)\mathbf{z}^{T}(n),\end{aligned} \quad (9)$$

where μ, usually denoted as the step size parameter, is a small positive constant that governs stability and convergence speed of the adaptation algorithm. By applying the LMS algorithm in [20], the adaptive ILA-based DPD technique using LMS is described in Algorithm 1, where $F_{\mathrm{PA}}\{\cdots\}$ is the PA transfer function, modeled by a MP function or a device under test (DUT). It is worth noting that the MP models in [6] are used for the PA behavior modeling in the rest of this framework. The input and output waveforms of these models can be described by

$$y(n)=\sum_{k=1}^{N}\sum_{m=0}^{M}c_{km}x(n-m)|x(n-m)|^{k-1}, \quad (10)$$

where c_{km} are the model coefficients, and N and M are the nonlinearity order and memory depth, respectively. $x(n)$ and $y(n)$ are the input and ouput baseband waveforms of the PA, respectively.

Algorithm 1 Adaptive ILA-based DPD technique using LMS.

Output: $\omega^{T}(n)$ and $y(n)$
Initialize: $n=0$, $\omega(0)$, μ.
for $n=1$ `to` $L-1$ **do**
  $x(n)=\omega^{T}(n-1)\phi(n)$
  $y(n)=F_{\mathrm{PA}}\{x(n)\}$.
  $z(n)=\frac{y(n)}{G_0}$
  $z_p=\omega^{T}(n-1)\mathbf{z}(n)$
  $e(n)=x(n)-z_{\mathrm{p}}(n)$
  $\omega^{T}(n)=\omega^{T}(n-1)+\mu e(n)\mathbf{z}^{T}(n)$
End for

The LMS algorithm is simple in terms of implementation and widely used in active noise control applications. However, it usually has slow convergence since increasing the step size parameter leads to instability problems [21].

In order to speed up the convergence of the adaptation, the RLS algorithm is developed for predistortion. The RLS algorithm is derived by minimizing a weighted sum of the magnitude-squared errors

$$\zeta\,(n,\omega)=\sum_{l=0}^{n}\lambda^{n-l}|e(l,\omega)|^{2}, \quad (11)$$

where $e(l,\omega)$ is the prediction error given in (8) and $0<\lambda<1$ is the forgetting factor (or weighting factor) that gives exponentially less weight to the previous error samples. The formulation of the RLS algorithm in [20, 21] is applied to minimize the cost function $\zeta(n,\omega)$. Then, the adaptive ILA predistortion using RLS is described in Algorithm 2, where $\mathbf{I}$ and $\mathbf{P}(0)$ are the identity matrix and initial correlation matrix, respectively and ρ is a positive constant. The commonly chosen value of λ is in the range of $0.95 \le \lambda < 1$ and $\rho > 100\sigma_x^2$, where σ_x^2 is the variance of the input [20, 21].

Algorithm 2 Adaptive ILA-based DPD technique using RLS.

1: Output: $\omega^{\mathrm{T}}(n)$ and $y(n)$
2: Initialize: $n = 0, \lambda, \mathbf{P}(0) = \rho\mathbf{I}$
3: **for** $n = 1$ to $\mathrm{L}-1$ **do**
4: $\quad x(n) = \omega^{\mathrm{T}}(n-1)\phi(n)$
5: $\quad y(n) = F_{\mathrm{PA}}\{x(n)\}.$
6: $\quad z(n) = \frac{y(n)}{G_0}$
7: $\quad z_p = \omega^{\mathrm{T}}(n-1)\mathbf{z}(n)$
8: $\quad e(n) = x(n) - z_{\mathrm{p}}(n)$
9: $\quad \mathbf{k}(n) = \frac{\mathbf{P}(n-1)\mathbf{z}(n)}{\lambda+\mathbf{z}^{\mathrm{T}}(n)\mathbf{P}(n-1)\mathbf{z}(n)}$
10: $\quad \mathbf{P}(n) = \frac{1}{\lambda}\left[\mathbf{P}(n-1) - \mathbf{k}(n)\mathbf{z}^{\mathrm{T}}(n)\mathbf{P}(n-1)\right]$
11: $\quad \omega(n) = \omega(n-1) + \mathbf{k}(n)e(n)$
12: **End for**

The choice of λ plays an essential role in order to effectively track the variation of PA characteristics. The smaller value of λ, the quicker the information in previous data will be forgotten. In other words, if λ is small and less than 1, the RLS algorithm becomes more sensitive and the oscillation of the parameter estimations changes quickly and become bigger [18], which linearizes the nonlinear behavior of PAs ineffectively. Hence, in order to make the parameter estimations more consistent and accurate in the steady state region, we propose an adaptive ILA based DPD technique using RPEM with the time-varying forgetting factor, which can improve the transient behavior of the algorithm.

2.3 Proposed adaptive ILA linearization using RPEM

The coefficient vector ω of the predistorter is estimated by using the Gauss-Newton RPEM algorithm [18] that minimizes the following cost function.

$$f_L(\omega) = \lim_{L\to\infty}\frac{1}{L}\sum_{l=1}^{L} E\left\{e^2(l,\omega)\right\}, \tag{12}$$

where $e(l,\omega)$ is given as in (8).

The formulation of the RPEM algorithm is derived in [18], which requires the negative gradient of $e(l,\omega)$ with respect to ω. From (8), the negative gradient is given by

$$-\frac{\partial e(n,\omega)}{\partial\omega} = \mathbf{z}^T(n). \tag{13}$$

When applying the RPEM algorithm [18] for PA linearization, the adaptive ILA-based DPD using RPEM algorithm is described in Algorithm 3, where ρ also is a positive constant and $\lambda(n)$ is a time-varying forgetting factor that tends exponentially to 1 as $n \to \infty$. In this algorithm, λ_0, $\lambda(0)$ and $\mathbf{P}(0)$ are initial variables designed by users. Typically chosen values are $\lambda_0 = 0.99$ and $\lambda(0) = 0.95$ [18]. It is worth noting that the RLS algorithm, in Algorithm 2, can be obtained exactly from the RPEM algorithm in Algorithm 3, by setting $\lambda_0 = 1$ and $\lambda(0) = \lambda$. In other words, the RLS algorithm is a special case of the RPEM algorithm.

Algorithm 3 The proposed adaptive ILA-based DPD technique using RPEM.

1: Output: $\omega^{\mathrm{T}}(n)$ and $y(n)$
2: Initialize: $n = 0, \lambda_0, \lambda(0), \mathbf{P}(0) = \rho\mathbf{I}$.
3: **for** $n = 1$ to $\mathrm{L}-1$ **do**
4: $\quad x(n) = \omega^{\mathrm{T}}(n-1)\phi(n)$
5: $\quad y(n) = F_{\mathrm{PA}}\{x(n)\}.$
6: $\quad z(n) = \frac{y(n)}{G_0}$
7: $\quad z_p = \omega^{\mathrm{T}}(n-1)\mathbf{z}(n)$
8: $\quad e(n) = x(n) - z_{\mathrm{p}}(n)$
9: $\quad \lambda(n) = \lambda_0\lambda(n-1) + 1 - \lambda_0$
10: $\quad \mathbf{k}(n) = \frac{\mathbf{P}(n-1)\mathbf{z}(n)}{\lambda(n)+\mathbf{z}^{\mathrm{T}}(n)\mathbf{P}(n-1)\mathbf{z}(n)}$
11: $\quad \mathbf{P}(n) = \frac{1}{\lambda(n)}\left[\mathbf{P}(n-1) - \mathbf{k}(n)\mathbf{z}^{\mathrm{T}}(n)\mathbf{P}(n-1)\right]$
12: $\quad \omega(n) = \omega(n-1) + \mathbf{k}(n)e(n).$
13: **End for**

2.4 Figure of merit

It is crucial that the evaluation criteria should be adopted to clearly validate the performance of PA behavioral modeling and DPDs. The most commonly used criteria are normalized mean square error (NMSE) in time domain, adjacent channel power ratio (ACPR) in frequency domain, and error vector magnitude (EVM) that are defined as in [4, 22].

The NMSE is an estimator of the overall difference between the predicted and measured signals in time domain. It is often defined in decibels as

$$NMSE = 10\log_{10}\left(\frac{\sum_{n=1}^{N}(|y[n]-x[n]|)^2}{\sum_{n=1}^{N}(|x[n]|)^2}\right), \tag{14}$$

where $x(n)$ is the experimental output (or desired output) of the DUT, and $y(n)$ is the output obtained from the model.

ACPR is the ratio between the total adjacent channel powers to the main channel signal power. It describes the degree of the signal regrowth into neighbouring channels. Since the ACPR characterizes the maximum power allowed

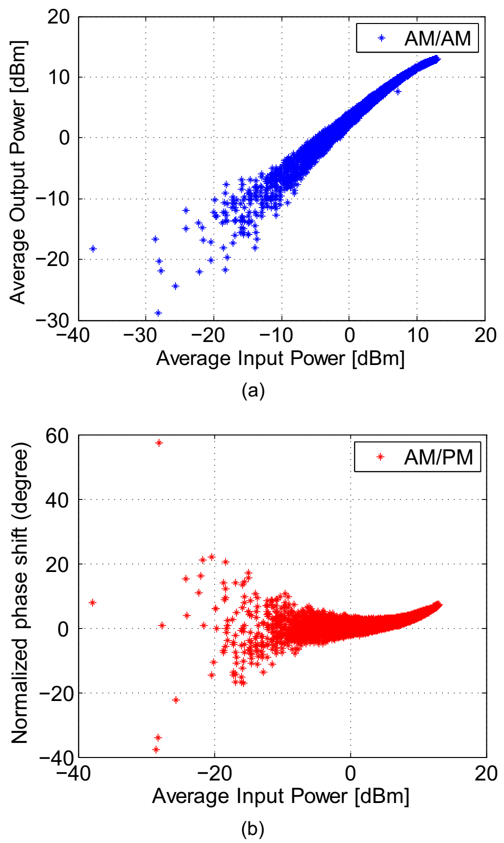

Fig. 2 The PA characteristics: **a** AM/AM. **b** AM/PM

to be radiated outside the allocated band, it plays a very important role in wireless radio standards. The ACPR is often expressed in decibels as

$$ACPR = 10\log_{10}\left(\frac{\int_{B_{adj}} |Y(f)|^2}{\int_{B_{ch}} |Y(f)|^2}\right) \tag{15}$$

where $|Y(f)|$ denotes the power spectrum of the measured output signal $y(n)$, B_{adj} and B_{ch} refer to the bandwidth of the adjacent and main channels, respectively (Figs. 2 and 3).

The EVM is a measure criterion that quantifies the imperfection to the output signal when compared to the

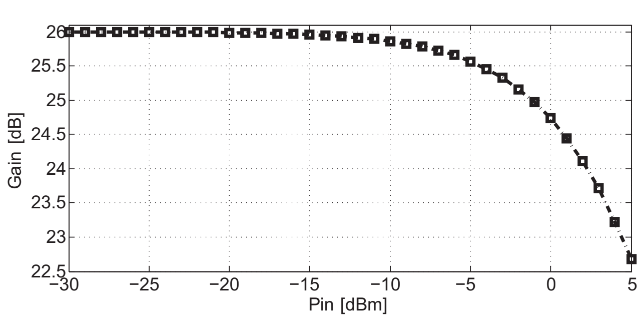

Fig. 3 Gain versus average input power of simulated PA

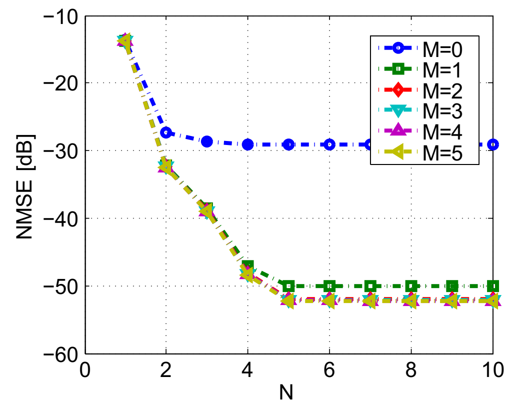

Fig. 4 NMSE versus N and M

input one. It describes the in-band distortion of the PA and is defined as

$$\mathrm{EVM} = \sqrt{\frac{\sum_{j=0}^{L}\left[\left(I_j - \hat{I}_j\right)^2 + \left(Q_j - \hat{Q}_j\right)^2\right]}{\sum_{j=0}^{L}\left[I_j^2 + Q_j^2\right]}} \tag{16}$$

where I_j and Q_j are the ideal output signal in-phase and quadrature components, and $\hat{I}_j$ and $\hat{Q}_j$ are their output measured counterparts, respectively.

3 Simulation results

In order to demonstrate the efficiency of the proposed DPD linearization method, we tested a simulated PA that is modeled by a Wiener model consisting of a FIR filter followed by memoryless nonlinearity model. The coefficients of the FIR filter are as in [23–25]

$$h_0 = 0.7692, h_1 = 0.1538, h_2 = 0.0769. \tag{17}$$

For the memoryless nonlinearity model, we use Saleh's model [26] which is defined by

$$y(n) = \frac{\alpha_a |v(n)|}{1 + \beta_a |v(n)|^2} e^{j\angle\left[v(n) + \frac{\alpha_\varphi |v(n)|^2}{1+\beta_\varphi |v(n)|^2}\right]}, \tag{18}$$

with

$$v(n) = h_0 x(n) + h_1 x(n-1) + h_2 x(n-2), \tag{19}$$

Table 1 Initialization of the various adaptive algorithms in ILA

	λ_0	$\lambda(0)$	λ	μ	$\mathbf{P}(0)$	$\omega(0)$
RPEM	0.99	0.95	–	–	$10^5\mathbf{I}$	$[1, 0, \cdots, 0]^T$
RLS	–	–	0.99 –	–	$10^5\mathbf{I}$	$[1, 0, \cdots, 0]^T$
LMS	–	–	–	0.02	–	$[1, 0, \cdots, 0]^T$

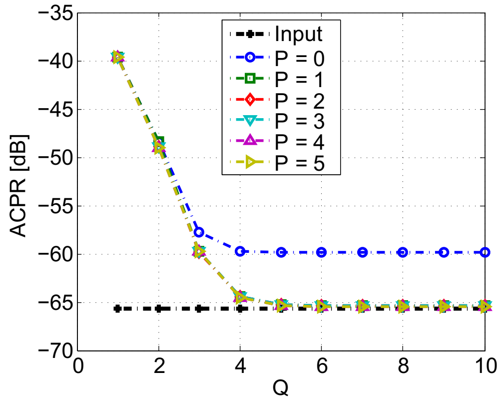

Fig. 5 NMSE versus Q and P

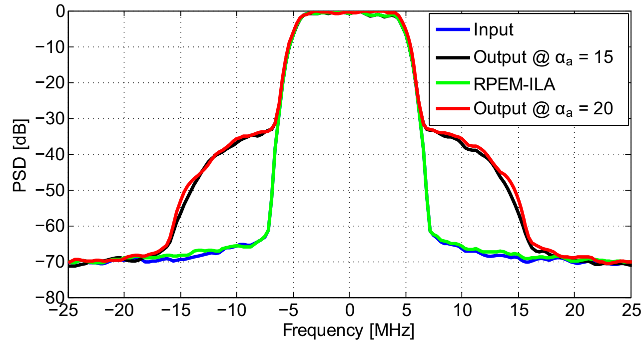

Fig. 7 Effectiveness of the proposed predistortion in suppressing spectral regrowth for the 16QAM signal with 10 MHz bandwidth and the power of −4 dBm when the PA characteristics change

where $x(n)$ and $y(n)$ are the input and output of the simulated PA, respectively, and $v(n)$ is the input of Saleh model. The parameters of Saleh model are as in [23]

$$\alpha_a = 20, \beta_a = 2.2, \alpha_\varphi = 2, \beta_\varphi = 1. \tag{20}$$

The transmitted symbols are modulated by 16-QAM with a bandwidth of 3.84 MHz. The input modulated signal is filtered by a raised cosine pulse shaping filter with roll-off factor of 0.22.

The MP model, expressed in (10), is used to model nonlinear behavior of the PA. In order to reduce the computational complexity, the orders (N and M) of the MP model are optimized by using a performance-based sweeping method [19]. Figure 4 shows the NMSE performance versus the orders of the PA model. From this figure, we can see that the optimal values of N and M are $N = 5$ and $M = 2$, respectively, in order to achieve a good trade-off between the best NMSE and the computational complexity.

The adaptive RPEM, RLS, LMS algorithms are initialized as in Table 1, where the initial weight vectors $\omega(0)$ have a first element as 1 and the others as 0. To effectively implement the ILA-based DPD technique, the orders (Q and P) of the PD and postdistorter models need to be optimized by evaluation of the ACPR performance after DPDs. In this simulation, the ACPR values are measured at the upper adjacent channels, corresponding to frequency offsets of 5 MHz. The ACPR performance obtained by the proposed RPEM-ILA is shown in Fig. 5. Obviously, we can observe that the optimal values of Q and P are 5 and 2, respectively, in order to obtain the ACPR value almost equal to that of the input. By applying the aforementioned optimization method to RLS-ILA and LMS-ILA linearizations, the optimal values of the PD models are also $Q = 5$ and $P = 2$, respectively.

The AM/AM and AM/PM characteristics computed at the instantaneous samples of the PA input and output, are shown in Fig. 2. It is clear that the simulated PA suffers from the nonlinearity and memory effects. Figure 3 shows the gain performance of the simulated PA with the average input power. One can observe that the gain in linear region is about 26 dB. The average input power at 1 dB compression

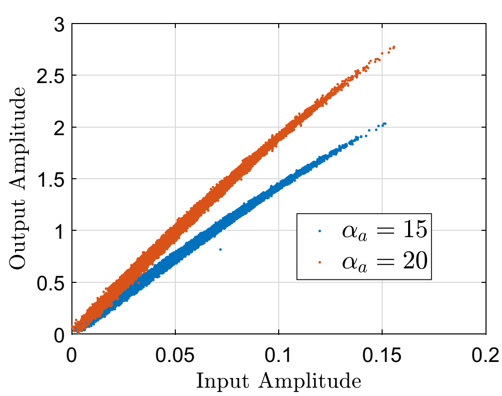

Fig. 6 AM/AM characteristics of the PA

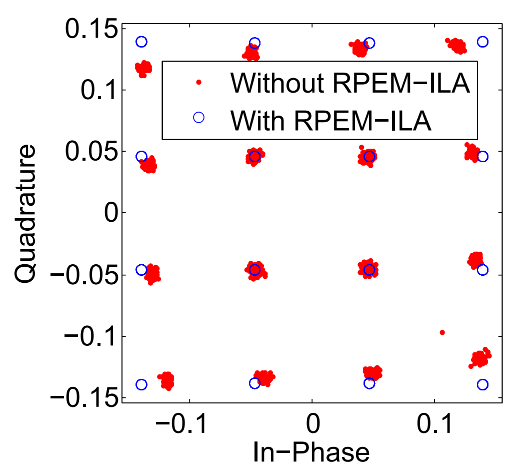

Fig. 8 Signal constellations before and after proposed RPEM-ILA linearization for the 16QAM signal with 10 MHz bandwidth and the power of −4 dBm

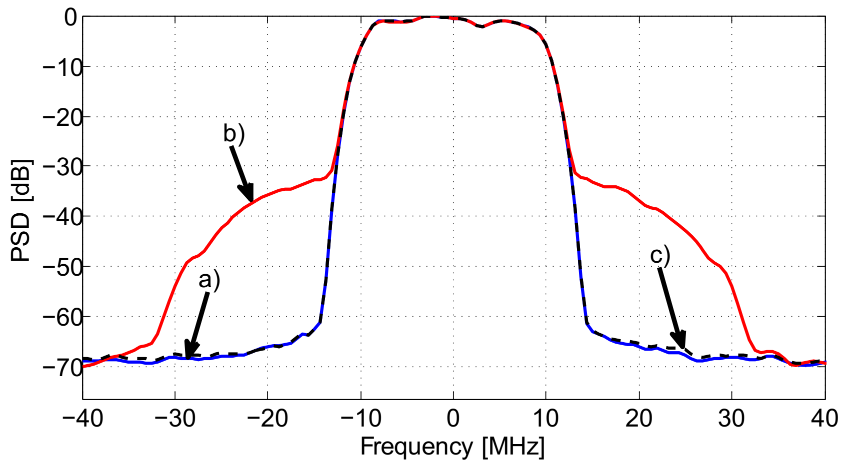

Fig. 9 Effectiveness of the proposed predistortion in suppressing spectral regrowth for the 32QAM signal with 20 MHz bandwidth and the power of −4 dBm: **a** PA input, **b** PA Output, **c** proposed RPEM based ILA

point and at 3 dB are around −1 dBm and 4.3 dBm, respectively.

We first investigate the effectiveness of the proposed DPD using the adaptive RPEM algorithm for the different types of the input signals and the variation of the PA characteristics. In order to characterize the variation of PA characteristics, the following parameters are changed in Saleh model:

$$\alpha_a = [15, 20]. \quad (21)$$

A 16QAM signal with 10 MHz bandwidth and the power of −4 dBm, is used to test our solution. Figure 6 shows the AM/AM characteristics of the simulated PA. Obviously, the PA behavior changes when α_a is varied. Figure 7 illustrates the power spectral density (PSD) before and after the proposed predistorter. Spectral regrowth is almost fully suppressed due to the changes in PA characteristics when the parameters of Saleh model are modified. The signal constellations of the PA output before and after DPD, are shown in Fig. 8. Because of memory effect, the PA output without linearization has the actual constellation points deviated from the ideal locations, resulting in the constellation distortion (or dispersion). It has an EVM of 6.75%. After employing the proposed predistorter, constellation distortion is effectively compensated and the corrected PA output has an EVM of 1.20%, making it an EVM improvement of 5.55%. Consequently, the proposed approach can effectively work for PAs with significant memory effects.

In order to keep the same parameters of Saleh model in [23], α_a is set at 20 for the remaining computer simulations. The proposed approach is also validated for the input with higher bandwidth and diverse modulation scheme. The result is shown in Fig. 9. We still observe significant reduction in spectral regrowth after the proposed predistorter. Figure 10 presents the constellation diagram of the PA output with and without the proposed DPD. Again, due to the memory effect, dispersion appears in the constellation, causing in-band distortion. Without

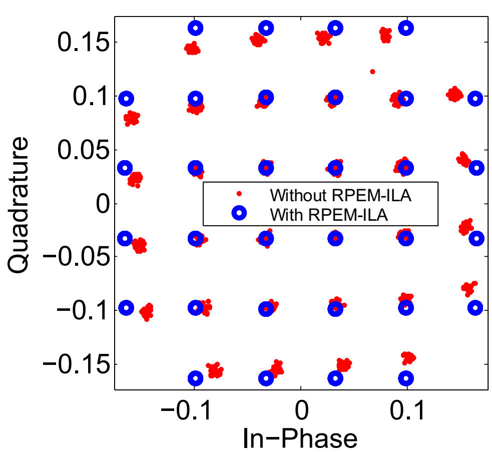

Fig. 10 Signal constellations with and without proposed RPEM-ILA linearization for the 32QAM signal with 20 MHz bandwidth and the power of −4 dBm

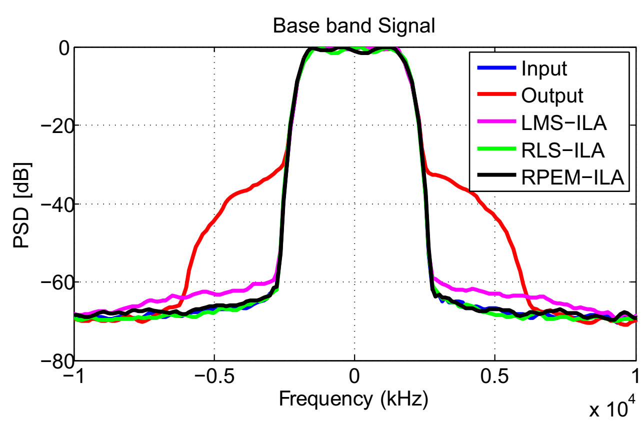

Fig. 11 Power spectral density (PSD) of the PA output before and after DPD using various adaptive algorithms with the input power of −4 dBm

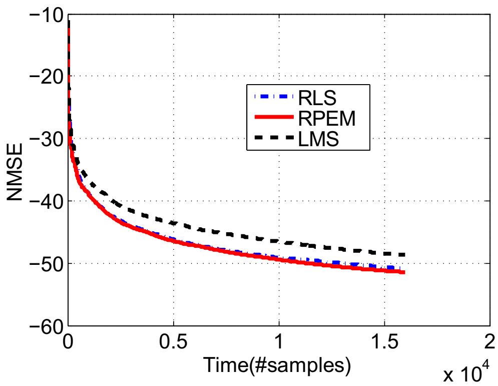

Fig. 12 Learning curves for different adaptive algorithms

linearization, the PA output has an EVM of 6.81%. When applying the proposed RPEM-ILA, it has the EVM of 0.8%, being equal to that of the input. The proposed RPEM-ILA obtains the EVM improvement of 6% and effectively corrects the constellation distortion (or dispersion).

We finally make the performance comparison between adaptive algorithms used in ILA based DPDs. In these simulations, a 16QAM signal with 3.84 MHz bandwidth and the power of −4 dBm, is used. Figure 11 shows an efficiency comparison in canceling the spectral regrowth between these algorithms for the input power of −4 dBm. It can be seen that there is a significant spectral regrowth reduction after DPDs. Both the RPEM and RLS algorithms obtain similar performance in terms of the spectral regrowth suppression, and get better than the LMS algorithm due to the fact that the achieved NMSE values by RPEM and RLS are almost identical and lower than those by LMS, as shown in Fig. 12. Thanks to the time-varying forgetting factor, the RPEM algorithm becomes less sensitive to noise and the coefficient estimates can approach the true values more rapidly with smaller oscillations than the RLS algorithm as shown in Fig. 13. In other words, the RPEM algorithm makes the parameter estimates more consistent and accurate than the RLS algorithm.

Figure 14a and b show the ACPR and EVM performance of the different adaptive algorithms for various input power levels, respectively. From these figures, one can observe that all linearization techniques show a significant performance improvement in terms of ACPR and EVM. The proposed adaptive RPEM-ILA obtains the ACPR values almost equal to those of input and shows similar ACPR values as RLS-ILA. It also gets around 5 dB of ACPR improvement better than LMS-ILA for the input power levels less than −4 dBm. Furthermore, after applying RPEM-ILA, the EVM values are significantly reduced and less than 0.26%, which shows

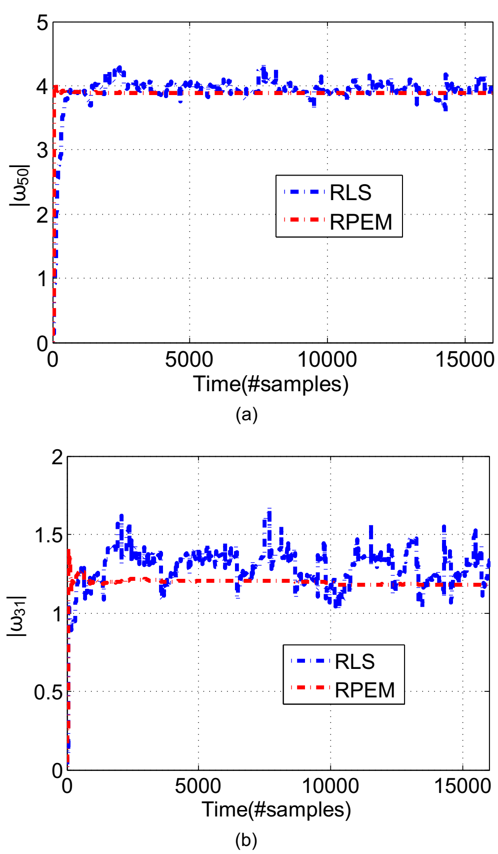

Fig. 13 Convergence behavior of the PD coefficient estimates. **a** ω_{50}. **b** ω_{31}

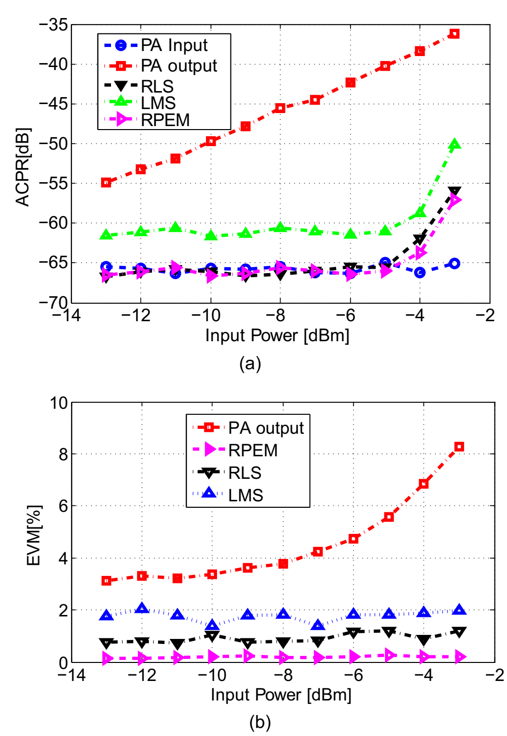

Fig. 14 ACPR and EVM performance after DPDs using various adaptive algorithms: **a** ACPR; **b** EVM

the better mitigation of in-band distortion than both LMS- and RLS-ILA. This is because the RPEM algorithm makes the PD coefficient estimates more consistent and precise in steady state as illustrated in Fig. 13. In other words, the proposed RPEM-ILA technique outperforms the compared ones.

4 Conclusions

In this paper, an adaptive ILA linearization using the RPEM algorithm has been proposed. Thanks to the time-varying forgetting factor, the PD coefficient estimates are consistent and accurate in steady state, leading to speed up the convergence, reduce the NMSE, and minimize the total nonlinear distortion at the PA output. The simulation results show that the proposed adaptive ILA using RPEM outperforms the one using either LMS or RLS. Moreover, the nonlinear distortion of the PA operated under different conditions (for example, the different input powers), can be almost fully compensated by employing the adaptive ILA with RPEM. In other words, the proposed DPD technique effectively linearizes the PA even if its characteristics change. So, this approach provides a very promising solution for the future wideband wireless communication systems where the PA characteristics change due to the type of signal, high-order modulation, working condition, etc. In the future work, we will consider the optimization and hardware implementation experiments as well as more efficient linearization methods by combining several techniques.

Acknowledgment This research is funded by Vietnam National Foundation for Science and Technology Development (NAFOSTED) under grant number 102.02-2016.12.

References

1. Chen Y, Guo Z, Yang X et al (2018) Optimization of coverage in 5g self-organizing small cell networks. Mobile Networks and Applications 23(6)
2. Ahn J, Lee J, Park S et al (2019) Power efficient clustering scheme for 5g mobile edge computing environment. Mobile Netw Appl 24(2)
3. Ghannouchi FM, Hammi O (2009) Behavioral modeling and predistortion. IEEE Microw Mag 10(7):52–64
4. Chani-Cahuana J, Landin PN, Fager C, Eriksson T (2016) Iterative learning control for RF power amplifier linearization. IEEE Trans Microw Theory Tech 64(9):2778–2789
5. Guan L, Zhu A (2014) Green communications: digital predistortion for wideband RF power amplifiers. IEEE Microw Mag 15(7):84–99
6. Ding L, Zhou GT, Morgan DR, Ma Z, Kenney JS, Kim J, Giardina CR (2004) A robust digital baseband predistorter constructed using memory polynomials. IEEE Trans Commun 52(1):159–165
7. Guo Y, Yu C, Zhu A (2015) Power adaptive digital predistortion for wideband RF power amplifiers with dynamic power transmission. IEEE Trans Microw Theory Tech 63(11):3595–3607
8. Schoukens M, Hammenecker J, Cooman A (2017) Obtaining the preinverse of a power amplifier using iterative learning control. IEEE Trans Microw Theory Tech 65(11):4266–4273
9. Zhou D, DeBrunner VE (2007) Novel adaptive nonlinear predistorters based on the direct learning algorithm. IEEE Trans Signal Process 55(1):120–133
10. Choi S, Jeong ER, Lee YH (2009) Adaptive predistortion with direct learning based on piecewise linear approximation of amplifier nonlinearity. IEEE Select Topics Signal Process 3(3):397–404
11. Suryasarman PM, Springer A (2015) A comparative analysis of adaptive digital predistortion algorithms for multiple antenna transmitters. IEEE Trans Circuits Syst I 62(5):1412–1420
12. Eun C, Powers EJ (1997) A new Volterra predistorter based on the indirect learning architecture. IEEE Trans Signal Process 45(1):223–227
13. Morgan DR, Ma Z, Ding L (2003) Reducing measurement noise effects in digital predistortion of RF power amplifiers. In: Proc IEEE International Conference on Communications (ICC'03), pp 2436–2439
14. Paaso H, Mammela A (2008) Comparison of direct learning and indirect learning predistortion architectures. In: Proc IEEE international symposium on wireless communication systems, pp 309–313
15. Hussein MA, Bohara VA, Venard O (2012) On the system level convergence of ILA and DLA for digital predistortion. In: Proc. 2012 international symposium on wireless communication systems (ISWCS), pp 870–874
16. Guan L, Zhu A (2011) Dual-loop model extraction for digital predistortion of wideband RF power amplifiers. IEEE Microwave and Wireless Components Letters 21(9):501–503
17. Mohr B, Li W, Heinen S (2012) Analysis of digital predistortion architectures for direct digital-to-RF transmitter systems. In: Proc. 2012 IEEE 55th international midwest symposium on circuits and systems (MWSCAS), pp 650–653
18. Söderström T, Stoica P (eds) (1989) System identification. Prentice-Hall Inc., Upper Saddle River
19. Abdelrahman AE, Hammi O, Kwan AK, Zerguine A, Ghannouchi FM (2016) A novel weighted memory polynomial for behavioral modeling and digital predistortion of nonlinear wireless transmitters. IEEE Trans Industrial Electron 63(3):1745–1753
20. Proakis JG, Manolakis DK (2006) Digital signal processing, 4th edn. Prentice-Hall Inc., Upper Saddle River
21. Haykin S (2014) Adaptive filter theory, 5th edn. Prentice-Hall Inc., Upper Saddle River
22. Mkadem F (2014) Behavioral modeling and digital predistortion of wide- and multi- band transmitter systems. Ph.D. dissertation
23. Feng X, Wang Y, Feuvrie B, Descamps A-S, Ding Y, Yu Z (2016) Analysis on LUT based digital predistortion using direct learning architecture for linearizing power amplifiers. EURASIP Wireless Commun Netw 2016(1):132
24. Kwon J, Eun C (2010) Digital feedforward compensation scheme for the non-linear power amplifier with memory. IJISTA 9:326–334
25. Eun C, Powers EJ (1995) A predistorter design for a memory-less nonlinearity preceded by a dynamic linear system. In: Proc. GLOBECOM '95, vol 1, pp 152–156
26. Saleh AAM (1981) Frequency-independent and frequency-dependent nonlinear models of twt amplifiers. IEEE Trans Commun COM-29(11):1715–1720

Affiliations

Duc Han Le[1] **· Van-Phuc Hoang**[1] **· Minh Hong Nguyen**[1] **· Hien M. Nguyen**[2] **· Duc Minh Nguyen**[3]

Duc Han Le
leduchan@gmail.com

Minh Hong Nguyen
nguyenhaihong2007@yahoo.com.vn

Hien M. Nguyen
nguyenminhhien2501@gmail.com

Duc Minh Nguyen
minh.nguyenduc1@hust.edu.vn

1 Le Quy Don Technical University, no. 236 Hoang Quoc Viet Str., Hanoi, Vietnam

2 Duy Tan University, Da Nang, Vietnam

3 Hanoi University of Science and Technology, no. 1 Dai Co Viet Str., Hanoi, Vietnam